Lidocaine carboxymethylcellulose with gelatine co-polymer hydrogel delivery by combined microneedle and ultrasound

Lidocaine carboxymethylcellulose with gelatine co-polymer hydrogel delivery by combined microneedle and ultrasound

Atul Nayak, Hiten Babla, Tao Han, Diganta Bhusan Das*

Department of Chemical Engineering, Loughborough University, Loughborough, LE11 3TU, UK

(*Corresponding Author; Email: D.B.Das@lboro.ac.uk; Tel: 0044 1509 22509;

Fax: 0044 1509 223923)

ABSTRACT

A study that combines microneedles and sonophoresis pre-treatment was explored to determine their combined effects on percutaneous delivery of lidocaine from a polymeric hydrogel formulation. Varying ratios of carboxymethylcellulose and gelatine (NaCMC:gel range are 1:1.60-1:2.66) loaded with lidocaine were prepared and characterised for zeta potential and particle size. Additionally, variations in the formulation drying techniques were explored during the formulation stage. Ex-vivo permeation studies using Franz diffusion cells measured lidocaine permeation through porcine skin after pre-treatment with stainless steel microneedles and 20 kHz sonophoresis for 5 and 10 minute durations. A stable formulation was related to a lower gelatine mass ratio because of smaller mean particle sizes and high zeta potential. Lidocaine permeability in skin revealed some increases in permeability from combined microneedle and ultrasound pre-treatment studies. Furthermore, up to 4.8 fold increase in the combined application was observed compared with separate pre-treatments after 30 minutes. Sonophoresis pre-treatment alone showed insignificant enhancement in lidocaine permeation during the initial 2 hours period. Microneedle application increased permeability at a time of 0.5 h for up to ~17 fold with an average up to 4 fold. The time required to reach therapeutic levels of lidocaine was decreased to less than 7 minutes. Overall, the attempted approach promises to be a viable alternative to conventional lidocaine delivery methods involving painful injections by hypodermic needles. The mass transfer effects were fairly enhanced and the lowest amount of lidocaine in skin was 99.7% of the delivered amount at a time of 3 hours for lidocaine NaCMC/GEL 1:2.66 after low frequency sonophoresis (LFS) and microneedle treatment.

Keywords Carboxymethylcellulose, gelatine**,** microneedles, sonophoresis, lidocaine, percutaneous

Abbreviations: Degree of substitution (D.S.), sodium carboxymethylcellulose (NaCMC), gelatine (gel)

1. Introduction

This paper is concerned with the delivery of lidocaine, a common anaesthetic, from a lidocaine carboxymethylcellulose with gel co-polymer hydrogel formulation such as discussed recently by Nayak et al. (2013). An ideal anaesthetic can be described as one that provides rapid, prolonged and effective localised anaesthesia via a mechanism of blocking sensory nerve fibres in the

periphery that induces no pain and causes no adverse local tissue reaction (Rudin, 2013; Richards and McMahon, 2013; Milewski and Stinchcomb, 2011). Lidocaine hydrochloride is a water soluble weak acid, fully ionised at pH 5.0 and administered into the plasma rich layer under the skin surface (González-Rodríguez et al., 2013; Igaki et al., 2013). However, this administration is conventionally performed via hypodermic needles as a low cost and fast acting method (Kim et al., 2012; Hedge et al., 2011). This is known to cause significant pains (Scarfone et al., 1998). Alternatives, such as eutectic mixture of local anaesthetics (EMLA), a topical form to administer lidocaine, require at least an hour of application to achieve effective analgesia, thus limiting its use especially in emergency situations (Nayak and Das, 2013). Therefore, there are important rationales for the pursuits of alternative lidocaine administration (Nayak et al., 2013; Nayak and Das, 2013). This can be evidenced in the European paediatric drug legislation which backs innovative approaches to develop ‘easy to administer’ and ‘minimally invasive’ drug delivery methods (Shah et al., 2011). The alternative rationales for lidocaine delivery include the need for increased safety amongst the patients and healthcare providers, increased compliance with those who possess a fear of needles, reduced discomfort and pain especially in the case of applying anaesthetics as well as improved ease of delivery (Gill and Prausnitz, 2007; Giudice and Campbell, 2006; Li et al., 2010). Oral administration can overcome many of the disadvantages associated with direct injection of drugs (Bal et al., 2010). However, one constraint is low bioavailability of some drugs which limits the effectiveness as therapeutic targets (Shipton, 2012; Benet et al., 1996; De Boer et al., 1979; Huet and Lelorier, 1980). Lidocaine’s oral bioavailability is approximately reduced by 65 - 96%, mainly by hepatic enzymes (Fasinu et al., 2011; Fen-Lin et al., 1993). In principle, innovative percutaneous delivery method could be used to overcome the barriers associated with direct injection and oral administration of drugs (Polat et al., 2011) such as lidocaine. The rate of passive diffusion (PD) of drugs by percutaneous delivery depends on the molecular structure, size and hydrophobicity in conjunction with the drug concentration gradients. However, many studies have used combinations of PD and non-invasive techniques with varying success, e.g., microneedles and ultrasound (Han and Das, 2013; Chen et al., 2010). This is the topic of this paper and it is discussed in more detail below.

Microneedles are needle-like structures of the size order of microns commonly arranged in a matrix (Gill and Prausnitz, 2007; Zhang et al., 2014; Olatunji et al., 2014). The geometry of microneedle influences its ability to pierce the skin but importantly, it can be designed to control/optimise the rate of drug delivery. The lidocaine NaCMC/GEL hydrogels pseudoplasticity permits the viscous formulation in allowing seepage into microneedle cavities to bypass the stratum corneum skin layer compared with passive diffusion (Nayak et al., 2013). Research has shown that a significant increase in skin permeability can be achieved when optimised microneedle arrays are used where the important factors include microneedle length, number of microneedles, the length and width aspect ratio and surface area of the microneedle patch (Al-Qallaf and Das, 2008; Al-Qallaf and Das, 2009; Olatunji et al., 2012; Olatunji et al., 2013; Guo et al., 2013). It has been suggested that

microneedles can be adapted to aid lidocaine delivery yielding many fold increase in delivery rate (Kwon, 2004; Li et al., 2008; Wilson et al., 2008; Kochhar et al., 2013; Ito et al., 2013; Zhang et al., 2012; Zhang et al., 2012; Nayak et al., 2013).

In a recent review paper, Nayak and Das (2013) have discussed the possibility of delivering lidocaine using biodegradable micro-needles. In exploring alternative applications of microneedles, a number of other studies have successfully delivered numerous active molecules using microneedles, e.g., hepatitis B vaccine (Guo et al., 2013), Solaraze® gel in extending pore opening (Ghosh et al., 2013b) and naltrexone co-drug with diclofenac drug (Banks et al., 2013). In another recent study, it has been shown that microneedles can be combined with ultrasound for increasing the delivery rate of a large macromolecular drug (Han and Das, 2013). These studies have further raised the hypothesis that microneedles and ultrasound combination could be used for greater epidermal lidocaine delivery in order to determine the significance of optimum sonophoretic power related the effects on lidocaine permeation.

In this context, it is important to state the classification of sonophoresis which is generally based on the frequency of ultrasound. The low frequency sonophoresis (LFS) is defined to be within the range of 20-100kHz and the high frequency sonophoresis (HFS) is usually for above 0.7MHz (Polat et al., 2011). The mechanism by which enhanced permeability is achieved via ultrasound can be linked to a number of physical phenomena including thermal effects, formation of cavitation, mechanical effects and convective localised fluid velocities in skin (Lavon and Kost, 2004). However, in the ultrasound pretreatment experiment, it is generally accepted that inertial cavitation is the largest contributor to the enhancement in skin permeability. It is more so with LFS as shown by Merino et al (2003) due to larger bubble size at low frequency range. Inertial cavitation occurs due to pressure variations induced by ultrasound, resulting in rapid growth and collapse of bubbles formed in the coupling medium. The collapsing of the aforementioned bubbles near skin surface will cause micro-jets due to asymmetrically release of energy. These micro-jets have been confirmed as the main contributors to the permeability increment (Wolloch and Kost, 2010). The effects of ultrasound have been studied for the enhancement of transdermal lidocaine administration with significant enhancement demonstrated with both pulsed and continuous output mode of LFS (Ebrahimi et al., 2012). However, as far as we are aware of, these techniques are yet to be combined and studied for permeability enhancement levels, particularly for lidocaine.

The potential for adapting microneedles for lidocaine delivery via hydrogel microparticles has been discussed previously with the conclusion that there is significant commercial potential for lidocaine microneedle products (Zhang et al., 2012; Nayak et al., 2013). Polymeric hydrogel microparticles are good for the purpose of controlling spreading (i.e., controllable spreading radius, droplet height and contact angle) of the drug formulation over skin (Nayak et al., 2013). A hydrogel drug vehicle comprises the electrostatic polyionic interaction of a branched structural polymer with a relatively

linear polymer in the formation of a cross-linked matrix to encapsulate Lidocaine molecules (Zhao et al., 2006; Lastumäki et al., 2003).

In this particular study, the drug vehicle for lidocaine encapsulation is polyanionic, carbohydrate based NaCMC crosslinked with polycationic, protein based gel in forming a hydrogel (Nayak et al., 2013). Previously lidocaine formulation bypassing the stratum corneum (SC) epidermal layer was outlined, the viscoelastic properties in adapting a NaCMC/gel network hydrogel prevents slippage of the drug formulation when applied to the skin and the possibility of non-convective flow through the opened cavities of the skin from microneedle treatment (Milewski and Stinchcomb, 2011; Ghosh et al., 2013a). To try and exploit this potential the main aim of the study is to combine the techniques in microneedle array and ultrasound technology as a pre-treatment to meet the definition of an ideal anaesthetic delivery method. Furthermore, this study will focus on using solid microneedles utilising the 'poke and patch' technique. The main advantage of this approach is the technical simplicity required for reproduction of the required micro-needles leading to reduction of cost. The other major advantage is that an extended release is possible using this approach. A carbohydrate based visceral hydrogel formulation was prepared as a model anaesthetic as this provides flexible properties and ability to encapsulate considerable amounts of liquid drug, lidocaine in this instance (Milewski and Stinchcomb, 2011), as discussed in the following section. Furthermore, the spreading behaviour of the prepared formulation was studied and compared with the spreading behaviour lidocaine solution as a Newtonian liquid. Unlike numerous studies performed using synthetic substrates, this study implements porcine skin as a lipophilic substrate as was attempted by Chow et al. (2008).

2. Materials and methods

NaCMC and gel emulsion was crosslinked to form hydrogels with encapsulated lidocaine in batch scale production. This formulation setup is highly beneficial because of fairly efficient preparation times in achieving a finished drug formulation and low heat treatment in adaptation of green chemistry.

2.1 Materials and equipments

Sodium carboxymethylcellulose (D.S. 0.9; M.W. 250kD), sorbitan mono-oleate (SPAN 80), glutaraldehyde 50% w/w, paraffin liquid (density range: 0.827-0.89 g/ml), lidocaine hydrochloride (M.W. 288.81 g/mol), methylene blue (50 % v/v) and porcine gelatine (type A) were purchased from Sigma Aldrich Ltd (Dorset, UK). Analytical grade acetic acid, high performance liquid chromatography (HPLC) grade acetonitrile and n-hexane (95% w/w) were purchased from Fisher Scientific UK (Loughborough, UK). A Gemini-NX column (C18) of particle size 3 µm was purchased from Phenomenex (Cheshire, UK) for HPLC instrumentation. Amputated porcine ears (age of pig: 5-6 months) were purchased from a local butcher and dissected into 20 mm x 20 mm squares before

storage at -20 ± 1ºC. Also 10 mm x 10 mm squares of same porcine skin were dissected as a substrate for droplet spreading. Microneedle patch (stainless steel, flat arrow head geometry and 1100µm length) was purchased from nanoBioSciences (Sunnyvale, CA, USA). Branson Digital Sonifier 450 (Danbury, USA) was chosen as the ultrasound output system. This ultrasound system includes an auto-calibrated transducer and a digital output controller. The frequency of the ultrasound is fixed at 20 kHz but the output powers are adjustable between 4 and 400 W. The equipment for droplet spreading studies were AVT Pike F-032 high performance camera (Allied Vision Technologies UK), Camera i-speed LT high speed video (Olympus, UK),

2.2 Formulation of lidocaine NaCMC:gel hydrogel

Paraffin oil (100 ml) was sheared continuously for up to 400 rpm in a stirred vessel bought from IKA (Staufen, Germany). Span 80 (0.5% w/w) was dispensed in ambient conditions. To this NaCMC (1.24 % w/w) in ultrapure water was added dropwise, and depending on the polymeric ratio (c % w/w), gel in ultrapure water was also added dropwise at 35-40ºC (Table 1). A subsequent pH reduction of the solution to pH 4.0 was performed by the addition of acetic acid (~3% w/w). While shearing at 400 rpm, lidocaine HCl (2.44 % w/w) was added dropwise in ultrapure water at 20°C into the polymer mixture. The polymeric mixture was then cooled to 5-10ºC for 30 minutes to initially harden the microparticles. Glutaraldehyde (0.11 % w/w) was added to the emulsion as a cross linker. Upon returning to 20°C temperature the hydrogel mixture was sheared for 2 hours at approximately 1000 rpm to ensure thorough mixing. The lidocaine NaCMC/gel formulation was then left to stand until a distinct w/o boundary was observed after which this formulation was left overnight at 1-5ºC. Excess paraffin liquid was removed via n-hexane separation shaking (50 % v/v); top organic layer was discarded before placing the hydrogel formulation in a vacuum oven (Technico, Fistreem International Ltd, Loughborough, UK) under full vacuum and a temperature of 20ºC for 8 hours. Following this, the formulation was washed with deionised (DI) water and filtered using commercial filter papers with pore size 6 µm (Whatman, Ltd, Oxon, UK) for removal of unbound lidocaine before further characterisation. In the case of F5 residual paraffin and n-hexane were removed by rotary evaporation (Heidolph Instruments, Essex, UK). Similarly, the formulation was washed with DI water and filtered as previously outlined.

Table 1

2.3 Zeta potential of lidocaine NaCMC:gel hydrogel

The zeta potential was measured using a Zetasizer (3000 HSa, Malvern Instruments, Worcestershire, UK). Lidocaine NaCMC/gel (2.0 ± 0.5 g/ml) in DI water was injected into the sample port, temperature maintained at 25.0°C and the results were obtained in triplicate. The zeta-potential (ζ) was measured in terms of electrophoretic mobility (µ) via an optical technique, and ζ (mV) (Park et al., 2005) of the diluted hydrogel was computed from the Smoluchowski equation (2) where µ is referenced with latex ($m^2\ v^{-1}\ s^{-1}$), η is the DI volume viscosity ($m^2 s^{-1}$), ε_o and ε_r are the permittivity in a vacuum and relative permittivity of DI water as medium respectively (Sze et al, 2003).

$$\zeta = \frac{4\pi\mu\eta}{(\varepsilon_r\varepsilon_o)} \quad (2)$$

2.4 Viscometric analysis of lidocaine NaCMC:gel hydrogel

A well-mixed sample volume (25 ml) of lidocaine NaCMC/gel hydrogel sample was determined for variations to viscoelastic properties at standard temperatures of 20°C. An inducing shear rotating viscometer (Viscotester VT550, Haake, Germany) with rotor and cup (NV1) assemblies and a constant ravine of 0.35 mm, in between the assembly was adapted in viscometric analysis. More details on this aspect of our work are presented by Nayak et al. (2013).

2.5 Optical micrographs of lidocaine NaCMC:gel hydrogel

Micrographs were obtained using an optical microscope (BX 43, Olympus, Southend-on-sea, UK) and a camera attachment captured coloured still images (Retiga-2000R, QImaging, British Columbia, Canada). Micrographs were pictured in triplicate for each formulation. An image processing software (*ImageJ)* was adapted in pixel measurement via graticule calibration to interpret particle size diameters from a random selection of 50 microparticles per image. ImageJ is a Java-based open source image processing and analysis program developed at the National Institute of Health (NIH), USA.

2.6 Controlled release of lidocaine from NaCMC/gel hydrogel

Lidocaine NaCMC/gel hydrogel (0.1 ± 0.05 g) was placed in an amber vial and 25.0 ml of DI water was dispensed before the sample was placed in a pre-heated thermo-stat bath at 37.0 ± 0.5°C (Grant Instruments, Cambridge, UK). Subsequently 1 ± 0.0005 ml of heated sample removed by autopipette (Eppendorf, Stevenage, UK), filtered using Nylon membranes (Posidyne, 0.1 µm) and analysed for lidocaine content using HPLC instrumentation. The results were measured in triplicate and the standard deviation from sample mean was taken.

2.7 Ex vivo skin permeation study of lidocaine NaCMC/gel hydrogel

Jacketed Franz diffusion cells (FDC) (Logan Instruments, New Jersey, USA) were used as previously annotated for determining the *ex vivo* drug permeation rate through porcine skin (Nayak et al., 2013). Porcine ear skin was used in this analysis because of the histological similarity with human skin. Dissected square skin sections (20 x 20 mm) were defrosted at 25°C for a maximum time of 1 hour before the commencement of this study. The FDC receptor chamber (5.0 ml) was filled with deionised water and constantly stirred using a magnetic flea. The FDC receptor volume was constantly maintained at 37 ± 1ºC through a water jacket. A square section of full thickness skin (subcutaneous fat and connective tissue removed) was placed on the top of the aperture surface of diffusion cell with a diffusion area of 1.33cm^2. The average skin thickness was recorded in the range of 760-787µm (± 25 µm). The continuous viscoelastic properties of skin are unlikely to allow for

microneedles to penetrate beyond 200 µm when considering 1500 µm needle length rollers penetrating a depth of 150µm (Roxhed et al., 2007; Badran et al., 2009). The lidocaine NaCMC:gel hydrogel (0.10 ± 0.03g) was placed on to the skin's donor compartment, the split second timer initiated and then the skin was securely clamped with a donor lid. A fixed 1.5ml receptor volume was syringe removed periodically from the receptor chamber and replaced with 1.5ml of deionised water. Following this the samples were analysed for free lidocaine using HPLC instrument (Agilent 1100 series, Hewlett Packard, U.S.). Similar FDC method was used for all drug release experiments concerning passive diffusion, microneedles only pre-treatment, LFS only pre-treatment, microneedles and LFS pre-treatment. Microneedles were carefully applied to the skin ensuring penetration and held in place using a constant pressure device comprising of a pneumatic piston (0.05MPa) for 3 or 5 minutes. LFS was supplied using a probe set to 20 kHz frequency for 5-10 minutes. Continuous application of ultrasound was implemented due to no significant difference being observed during pre-treatment applications (Herwadkar et al., 2012). The inter-coupling distance between the skin and probe was set to 2mm with coupling medium of deionised water. A minimum lidocaine concentration of 1.5 µg/ml was deduced from literature as the permissible effective drug therapeutic value in plasma (Schulz et al., 2012; Grossman et al., 1969).

2.8 Spreading of lidocaine NaCMC;gel 1:2.33 across porcine skin

The setup for measurement of spreading radius, droplet height and apparent contact angle of droplet was similar to Chao et al (2014). A square section of porcine skin (10 mm x 10 mm) was placed flat in a closed sample box. A sample droplet (3.0 ± 0.5µl) was dispensed on the porcine skin, camera frame rate capture of 1.85 frames per second (fps) was maintained and the results recorded. Results were obtained in duplicate for the optimum particle size controlled formulation and compared with a duplicate set of lidocaine solution of the same lidocaine loading weight (2.44 % wt).

2.9 Histological study

The determination of microneedle insertion depth into skin by post microneedle treatment of skin was adapted from Cheung et al (2014). First, the skin sample is pretreated using 1100 µm microneedle patch for 5 min. Then, the porcine skin sample is stained using methylene blue (50% v/v) and merged into embedding compound (Bright Cryo-m-Bed, Huntingdon, UK) which is filled in a cuboid mould. The whole sample is then put inside the microtome (Bright Cryostat 5030, Huntingdon, UK) to solidify. The frozen sample is cut into 15 µm slices and analysed under the microscope for the histology.

3. Results and discussions

3.1. Lidocaine NaCMC/gel hydrogel microparticle size diameters and morphology

Lidocaine encapsulated hydrogel microspheres based on NaCMC and gelatine were prepared using glutaraldehyde in transforming emulsion droplets to defined microparticles. As the mechanisms for ionic interactions in forming spherical microparticles are known (Gupta et al., 2000; Berger et al.,

2004), it is not discussed in detail in this paper. The morphological observations of lidocaine NaCMC:GEL microparticles are spherical, well-formed and slightly agglomerated for a significant number of them (Fig. 1a, 1b). Mean particle size diameters (Table 1) in the formulation ranged from 5.89-14.60µm depending on the formulation with an increase in mean particle size observed with an increased gelatine ratio. This is the likelihood of increased gelatine component of the hydrogel, producing larger droplets during the w/o emulsification and subsequent hardening after the addition of glutaraldehyde. The rotary evaporation method yielded significantly larger particle sizes in comparison to vacuum drying. Interestingly, a positively skewed particle size distribution was observed for all lidocaine hydrogel formulations (Fig. 2).

Fig. 1 Fig. 2

3.2. Dispersion of lidocaine NaCMC/gel hydrogel microparticles

Zeta potential studies in lidocaine NaCMC/gel hydrogels demonstrated a stable and fairly dispersed microparticulate system. The results (Fig. 3) expressed a trend of decreasing stability with an increase in the gelatine ratio, which in theory should impact a greater level of microparticle agglomeration thus likely affecting the permeability through skin. The pH of all formulations was kept constant and therefore it should not have affected the zeta potential although the slight decline of ζ-potential in the positive direction is linked to the increase in gelatine ratio caused by gelatine in conjunction to lidocaine possessing a positively charged tertiary amide group at pH 4.0 and thus contributing to the increasing negative surface charge. The anionic polymer, sodium carboxymethyl cellulose has a ζ-potential value of -30mV (Ducel et al., 2004) and electric charge neutralisation did not occur or was not significantly induced by gelatine or lidocaine, so the overall lidocaine NaCMC:gel hydrogel charge was greater than -30mV. Nevertheless, reduced agglomeration is the result of a medium pKa, higher dielectric constants in comparison to a polymeric hydrogel components converging to significantly low overall ζ-potential range of -35 to -40mV and effect of electrostatic particle repulsion (Xu et al., 2007).

Fig. 3

3.3. Viscoelasticity of lidocaine NaCMC/gel hydrogel

Viscosity determination (Fig. 4) revealed a lenient pseudoplastic nature for the formulation with lidocaine NaCMC/gel hydrogel with good correlative best fit curves observed for individual set of data points ($R^2 > 0.93$). The dynamic viscosity plots showed similar mild pseudoplastic behaviour between the formulations with lidocaine NaCMC/gel 1:2.66 hydrogel being marginally higher when considering the upper viscosity range of 0.5 to 0.6 Pa.s at a starting shear of 25 s^{-1} and then more defined shear thinning behaviour observed above 100 s^{-1}. Lidocaine with sodium carboxymethylcellulose as a polyanionic vehicle alone will not be sufficient in enhancing

pseudoplastic properties and a recent study has shown that the profile of a dynamic viscosity plot is Newtonian (Alaie, 2013).

Fig. 4

3.4 Control of lidocaine NaCMC:gel 1:2.33 spreading on porcine skin.

The spreading radius and height of lidocaine NaCMC/gel 1:2.33 outline significant control on its spreading behaviour compared with lidocaine solution of the same mass loading (Fig. 5a and 5b). The beginning of the plateau effect is observed after 10 seconds and therefore, there is expected to be a localisation effect on the skin surface (Fig. 5a and 5b). The apparent contact angles of lidocaine NaCMC/gel 1:2.33 droplets are considerably higher than the lidocaine solution contact angle droplets, near to the skin impact time of 0 seconds (Fig 5b). Apparent contact angle stability is noticed after 40 seconds (Fig. 5c). Our results also show that the lidocaine solution is a Newtonian liquid that can spread a much faster than lidocaine NaCMC/gel microparticles.

Fig. 5

3.5. The percentage release of lidocaine from controlled release of lidocaine.

All four lidocaine NaCMC/gel hydrogels outline rapid release of lidocaine directly in DI water during the first 1 hour with steady state conditions observed in the next three hours (Fig. 6a). A 0.3 fold decrease in cumulative release is observed in the first hour when comparing lidocaine NaCMC/gel 1:1.6 with lidocaine NaCMC/gel 1:2.66 as the highest releasing outline. Also, a 0.1 fold decrease in cumulative release was observed in the next three hours when comparing lidocaine NaCMC/gel 1:1.6 with lidocaine NaCMC/gel 1:2.66. This shows that the variation between hydrogel ratios is not significantly large as permeation release profiles explained in the following sections. The percentage release of lidocaine from NaCMC/gel hydrogels were determined by the following equation 1:

$$Percentage\ drug\ release = \frac{Ms-Mt}{Ms}\ x\ 100 \quad (1)$$

Where Ms is the maximum mean cumulative steady state concentration of drug and Mt is the mean cumulative concentration of lidocaine taken specifically at release time. The highest amount of Lidocaine released was from NaCMC/gel 1:1.6 hydrogel in which 32.3% was detected in the DI water media in one hour (Fig. 6b). This is because the smaller particles sizes of Lidocaine NaCMC/gel 1:1.6 ratio allow for a greater surface area and encapsulated lidocaine thus rapidly dissolves in DI water. The lidocaine NaCMC/gel 1:2.66 ratio comprises larger microparticles and therefore a smaller surface area is exposed for DI water dissolution so the percentage of lidocaine released was 17.4% in one hour. Significantly less amounts of lidocaine is released for all NaCMC/gel hydrogel formulations after 1 hour reflecting the steady state conditions of the hydrogel as the DI water media becomes a saturated solution.

Fig. 6

3.6 Histological analysis on the microneedles

The microneedles that are employed in the histological experiment are 1100 µm in length. The purpose of the histological experiment is to determine the insertion depth of this microneedle patch under thumb pressure for which post-microneedle treated skin is micrograph imaged (Fig. 7). According to Fig.7, the insertion depth is between 300 µm and 400 µm which are much lower than the real length of microneedles. This is caused by several reasons, such as the viscoelastic properties of the skin, the geometry of the microneedles and the insertion force. This reduced insertion depth can further affect the permeation results.

Fig. 7

3.7 Passive diffusion of lidocaine NaCMC/gel hydrogel

Skin passive diffusion experiments were carried out in order to provide a control from which any pre-treatment enhancement results can be compared and contrasted. The lowest polymeric microparticle ratio 1:1.6 of lidocaine (Fig. 8a) outlines the most desirable cumulative permeation for lidocaine in crossing the minimum threshold therapeutic level after 0.57 hours. This is the shortest lag time for reaching the pain receptors for lidocaine in the deep dermis region rich in watery plasma and nerves. The hydrogel microparticle chemistry is a combination of significantly high negative zeta potential and smaller mean particle size contributing to an increased permeation. All lidocaine NaCMC/gel ratio hydrogels have demonstrated a very low initial permeation at a maximum of 0.3µg/ml reached in 0.5 hours. This is the normal lag time because of a longer path length for microparticle permeation when considering the topmost SC layer surface area bigger than the accessible VE layer microcavities. However, lidocaine NaCMC/gel 1:2.0 and lidocaine NaCMC/gel 1:2.66 hydrogels are the next two favourables after the most desirable formulation containing a polymeric mass ratio 1:1.6 for bypassing the minimum therapeutic threshold at a shorter time interval. Initially, lidocaine is diffusing through the fresh skin because of microparticulate disruption to the hydrogel formula caused by natural skin moisture hence the low initial concentration rates proceeding upto 0.5 hours. Due to the requirements of lidocaine as an fast acting anaesthetic the current results confirm enhancement of permeation is required if minimum therapeutic threshold of lidocaine (1.5µg/ml) are to be reached within a suitable time frame for this technique to be of practical use. The lag time to cross a minimum therapeutic level is slightly greater than 1 hour in lidocaine NaCMC/gel 1:2.33 hydrogel and just over 2 hours for lidocaine NaCMC/gel 1:2.66 hydrogel, rotary evaporation method with respect to passive diffusion alone which is considerably a long, unreasonable waiting time for a promising polymeric hydrogel ointment drug. The cumulative lidocaine thresholds tend to stabilise post 4 hours, where equilibrium is reached and no more drug is

released into the concentrated dermal region. This means that the lidocaine hydrogel ointment can be washed off the skin. Lidocaine NaCMC/gel hydrogel was compared with lidocaine solution permeation from literature (Sekkat et al., 2004). Prior to this passive diffusion comparison with lidocaine solution passive diffusion, the permeation units of µg/ml were converted into µg/cm^2 by the product of the known receptor volume followed by the quotient of the adjustment factor value of 2.36 (3.14 cm^2/ 1.33 cm^2) due to the increase in FDC diffusion area when comparing a similar study using a smaller aperture diameter (Sekkat et al., 2004). The current lidocaine NaCMC/gel 1:1.6 hydrogel crosses the minimum therapeutic threshold by 1.8 fold than lidocaine solution on similar full thickness skin despite lidocaine solution permeating initially at 1.4 fold faster before a half an hour time frame and not anywhere near the minimum therapeutic threshold (Sekkat, 2004). Lidocaine NaCMC/gel 1:2.66 and lidocaine NaCMC/gel 1:2.66 hydrogel formulated by rotary evaporation were chosen to be studied for further enhancement via pre-treatment. The factor of permeation enhancement can be deduced when making this comparison.

Fig. 8

3.8 Ultrasound only pre-treatment of lidocaine NaCMC/gel ratio 1:2.66 hydrogel

To observe the effect of power and application time of LFS has on permeation, LFS was applied continuously with varying power and exposure time as shown in Fig. 8b. Theoretically, the exposure of LFS should form inertial cavities in the coupling medium and develop micro-jets toward the skin surface to aid permeation. However, lidocaine transport through the skin saw no significant enhancement up to 2 hours after which a significant enhancement, especially power induction, 18W at 10 mins for lidocaine NaCMC/gel 1:2.66 (T-test $P<0.026$) outlined a greater permeation profile. The results conclude that an increase in power has a greater enhancement effect compared to an increase in LFS exposure time; however, no significant increase in lidocaine transport through the skin was observed during the initial stages after varying respective power induction and time durations while maintaining constant NaCMC/gel ratios of lidocaine hydrogel drug application. It is predicted that a higher LFS power level would further increase diffusion; however, the risk of thermal effects would be too high for this to be of practical use.

3.9 Microneedle pre-treatment of lidocaine NaCMC/gel ratio 1:2.66 hydrogel

PD permeation (Fig. 8d) and microneedle assisted (MN) permeation (Fig. 8c) with a post application time limit of 3 and 5 minutes concurrently were compared altogether. Microneedle only pre-treatment of lidocaine NaCMC/gel 1:2.66 hydrogel generated a substantial increase in lidocaine permeation for both the 3 and 5 minute post MN duration (Fig. 8c). A statistically significant difference ($P<0.04$) was observed for MN application duration. Initial ($t=0.5h$) permeation for the 3 and 5 minute patch duration resulted in increases of 9 and 17 fold respectively. An average 3 fold increase in permeation was observed for the 3 minute microneedle application and comparatively an increase by 4 fold for a 5 minute microneedle application. The results indicate that therapeutic

levels of lidocaine could be reached within 0.15 hours or 9 minutes post application MN, in comparison to no pre-treatment requiring 40 minutes (Fig. 8c, 8d). The reason for this short lag time is due to lidocaine microparticles traveling at a shorter path length to the deep dermis layer. The stratum corneum layer has been bypassed by artificial microneedle cavities. Microneedle assisted cumulative release study with respect to lidocaine formulations has not been performed *ex vivo* to date. However, in vivo release studies have been performed using non degrading polymeric microneedle array coating of lidocaine alone, sustained approximately 15 minutes of delivery thus proven successful for rapid emergency anaesthesia (Zhang et al., 2012). In vivo release studies with *ex vivo* cumulative release studies are completely incomparable due to obvious differences in experimental procedures and removal of active drug for characterisation. The lidocaine NaCMC/gel 1:1.6 ratio (Fig. 8a) hydrogel crosses the therapeutic level at significantly slower time duration, greater than 30 minutes in lidocaine NaCMC/gel 1:2.66 ratio in comparison of microneedle and LFS treatment. This is due to the fact that microneedles and ultrasound are involved in either cavity engulfing of larger sized hydrogel microparticles.

3.10 Microneedle and ultrasound (dual) pre-treatment of lidocaine NaCMC/gel ratio 1:2.66 hydrogel

Both pre-treatments (dual) were combined and studied for further permeation enhancement in comparison to microneedle or LFS pre-treatment only. Lidocaine NaCMC/gel 1:2.66 hydrogel in which combining a 10 minute application of 18W LFS after a 5 minute application of microneedles demonstrated an initial faster permeation by 23 fold with an average 4.8 fold increase over 30 minutes of application when compared with separate device treatments and passive diffusion (Fig. 8d). Therapeutic levels of lidocaine could theoretically be reached after 7 minutes post application in terms of reaching the deep dermis layer of skin as the target. A general increase in permeation throughout the period of experimentation can be noticed rather than post 2 hours as seen with LFS pre-treatment only, this could be due to efficiency of LFS pre-treatment is further enhanced on porous skin sample formed via the microneedle patch.

3.11 Dual pre-treatment of lidocaine NaCMC/gel 1:2.66 hydrogel via rotary evaporation method

Lidocaine NaCMC/gel 1:2.66 hydrogel with the rotary evaporation method as described earlier, favoured an additional time of nearly 0.9 hour or fifty minutes after the application of 18W LFS at 10 minutes ($P < 0.04$) to reach minimum therapeutic level in conjunction to a two fold average increase in permeation after 1 hour, compared with the same formulation without rotary evaporation method (Fig. 8d, 8e). This was the likelihood of higher heating temperatures compromising the glutaraldehyde fixation and thus resulting in larger microparticle as previously reported. Higher heating temperatures were required in the large volume removal of n-hexane and paraffin oil mixture by solvent evaporation. A 5 minute application of the microneedle array led to an initial increase by 2.8 fold and subsequently an average 3.4 fold increase was observed with respect to the deep dermis layer skin target. Combining the two pre-treatments resulted in an initial permeation

increase by 3.8 fold followed by an average increase by 4.1 fold in comparison to passive diffusion only (Fig. 8d, 8e). Therapeutic levels of lidocaine were reduced from just over 2 hours to less than 1 hour on average.

3.12 Mass transfer of lidocaine from NaCMC/gel 1:2.66 hydrogel

The percentage of lidocaine remaining inside *ex vivo* skin was determined by the subtraction of the mass of lidocaine initially encapsulated during formulated preparation (125000 µg) by the cumulative amount detected in DI water from controlled release studies. The purpose of using controlled release studies is to determine the amount of lidocaine contained in the vehicle as mass balance before the subtraction of the mass of lidocaine in the receptor in which the DI water in the receptor is the deep dermis. All mass balances were carried out in µg and converted from cumulative concentration units of µg/ml before the percentage of lidocaine remaining inside the skin was determined (Fig. 9). Overall the mass transfer of lidocaine with respect to all treatment applications appeared to outline a gradual, slow process of diffusing through the full thickness appendage. However there is a fairly substantial decline in the percentage of lidocaine remaining in the skin when microneedle and ultrasound treatment (LFS) method was applied. This can be interpreted as diffusion of lidocaine molecules through skin cells and layers before clearance into the blood stream. The lowest percentage of lidocaine remaining in the skin is 99.7 % after a time of 3 hours (Fig. 9).

Fig. 9

4 **Conclusions**

This study aimed to use low frequency sonophoresis and microneedles as a pre-treatment to skin in order to enhance permeation of lidocaine encapsulated in a formulation. A significantly more microparticle stability was found with lower gelatine ratios (1:1.60); however all formulations were sufficiently stable (zeta potential: ≥ -30mV). Our diffusion experiments revealed a small increase in diffusional permeation when low frequency sonophoresis was used in combination with a microneedle array pre-treated skin. However, rotary evaporation during the final polymeric drug formulation stage caused significant reductions in lidocaine permeation levels. Nota bene that the main purpose for utilising rotary evaporation was for reduced time in removal of a large volume of residual paraffin and n-hexane as the final operative method compared to vacuum oven drying (data not shown). Lidocaine NaCMC/gel 1:2.66 and lidocaine NaCMC/gel hydrogel 1:2.66 formulated by rotary evaporation showed a decreased time required to reach minimum therapeutic levels of lidocaine by 5.7 and 2 fold, respectively. Generally, lidocaine permeation was significantly increased with higher sonophoresis power and increasing exposure duration demonstrated a minor increase of the permeation rate for lidocaine NaCMC/gel hydrogel formulations. Also the microneedle application time duration of 5 minutes resulted in a highly favourable increase in lidocaine permeation. Furthermore, combining microneedle and low frequency sonophoresis pre-treatments allowed for the time to reach minimum therapeutic lidocaine levels to be significantly reduced, For

example, in the case of lidocaine NaCMC/gel, 1:2.66 hydrogel therapeutic thresholds of lidocaine were reached within 7 minutes of application. The mass transfer effects in which the percentage of lidocaine remained in the full skin depicted the gradual movement of drug in targeting pain receptors below the SC layer. The lidocaine NaCMC/gel 1:2.66 hydrogel treated by microneedles and LFS shows a greater mass transfer profile. The US and MN treated lidocaine NaCMC/gel 1:2.66 has a 0.18 % mass transfer of lidocaine through skin within 2 hours compared with 0.01 % mass transfer of lidocaine through skin. Therefore, this method is promising and could be of medical use as a painless, easy to administer technique for drug delivery overcoming the time constraints associated with delivery of lidocaine. Lidocaine NaCMC/gel 1:2.66 hydrogel is likely to be the most desirable drug formulation candidate for further developmental studies reaching potentially important pre-clinical and final post clinical stage developments. In order to develop a less polydisperse but low micron scale lidocaine hydrogel formulation requires a longer time frame and added investment. The resources and materials in developing a lidocaine NaCMC/gel 1:2.66 hydrogel without rotary evaporation is economical on a batch scale at present. Lidocaine. NaCMC/gel 1:2.33 formulation with defined morphological appearance is able to remain on the surface of the skin for longer durations compared with a lidocaine solution of the same mass loading.

5. **Acknowledgements**

The authors acknowledge the help of Craig Chao for his assistance towards the characterisation of droplet spreading on skin (Figure 5).

6. **References**

Alaie, J., Vasheghani-Farahani, E., Rahmatpour, A., Semsarzadeh, MA. (2013). Gelation rheology and water absorption behavior of semi-interpenetrating polymer networks of polyacrylamide and carboxymethyl cellulose. *Journal of Macromolecular Science, Part B*, 52, 604-613.

Al-Qallaf, B., Das, D.B. (2009). Optimizing microneedle arrays to increase skin permeability for transdermal drug delivery. Annals of the New York Academy of Sciences, 1161, 83-94.

Al Qallaf, B and Das, DB (2008) Optimization of square microneedle arrays for increasing drug permeability in skin, *Chemical Engineering Science*, 63, 2523-2535, DOI: 10.1016/j.ces.2008.02.007.

Badran M.M, Kuntsche J., Fahr A. (2009) Skin penetration enhancement by microneedle device (Dermaroller®) in vitro: Dependency on needle size and applied formulation. European Journal of pharmaceutical Sciences, 36, 511-523.

Bal, S.M., Ding, Z., van Riet, E., Jiskoot, W., and Bouwstra, J.A. (2010). Advances in transcutaneous vaccine delivery: Do all ways lead to Rome? *Journal of Controlled Release*, 148, 266-282.

Banks, S.L., Paudel, K.S., Brogden, N.K., Loftin, C.D., and Stinchcomb, A.L. (2013). Diclofenac enables prolonged delivery of naltrexone through microneedle-treated skin. Pharmaceutical Research, 28, 1211-1219.

526 Benet, L,Z., Oie, S., and Schwartz, J.B. (1996). Design and optimisation of dosage regimens:
527 pharmacokinetic data. In J.G. Hardman, L.E. Limbard, P.B. Molinoff, R.W. Rudon, and A.G.
528 Gilman (Eds.), *The pharmacological basis of therapeutics* (pp. 1707-1792). McGraw Hill, New
529 York.
530 Berger, J., Reist, M., Mayer, J.M., Felt, O., Peppas, N.A., and Gurny, R. (2004). Structure and
531 interactions in covalently and ionically crosslinked chitosan hydrogels for biomedical
532 applications. *European Journal Pharmaceutics and Biopharmaceutics*, 57, 19-34.
533 Chao TZ, Trybala A., Starov V., Das D.B. (2014). Influence of haematocrit level on the kinetics of
534 blood spreading on thin porous medium during blood spot sampling. *Colloids and Surfaces A:*
535 *Physicochemical and Engineering Aspects*, 451, 38-47.
536 Chen, B., Wei, J., and Iliescu, C. (2010). Sonophoretic enhanced microneedles array (SEMA)—
537 Improving the efficiency of transdermal drug delivery. *Sensors and Actuators B: Chemical*, 145,
538 54-60.
539 Cheung K., Han T., Das D.B. (2014) Effect of force of microneedle insertion on the permeability of
540 insulin in skin. *Journal of Diabetes Science and Technology*. DOI: 10.1177/1932296813519720
541 (in press).
542 Chow KT, Chan LW, Heng PWS (2008) Characterization of spreadability of nonaqueous
543 ethylcellulose gel matrices using dynamic contact angle. Journal of Pharmaceutical Sciences
544 97: 3467-3481.
545 Davidson, A., Al-Qallaf, B., and Das, D.B. (2008). Transdermal drug delivery by coated
546 microneedles: Geometry effects on effective skin thickness and drug permeability. *Chemical*
547 *Engineering Research and Design*, 86, 1196-1206.
548 De Boer, A.G., Breimer D.D., Mattie, H., Pronk, J., and Gubbens-Stibbe, J.M. (1979). Rectal
549 bioavailability of lidocaine in man: partial avoidance of "first-pass" metabolism. *Clinical*
550 *pharmacology and therapeutics,* 26, 701-709.
551 Ducel, V., Richard, J., Saulnier, P., Popineau, Y., and Boury, F. (2004). Evidence and
552 characterization of complex coacervates containing plant proteins: application to the
553 microencapsulation of oil droplets. *Colloids Surface A*. 232, 239–247
554 Ebrahimi, S., Abbasnia, K., Motealleh, A., Kooroshfard, N., Kamali, F., and Ghaffarinezhad, F.
555 (2012). Effect of lidocaine phonophoresis on sensory blockade: pulsed or continuous mode of
556 therapeutic ultrasound? *Physiotherapy*, 98, 57-63.
557 Escobar-Chávez, J.J., Rodríguez-Cruz, I.M., and Domínguez-Delgado, C.L. (2012). Chemical and
558 physical enhancers for transdermal drug delivery. In Dr Luca Gallelli (Ed), *Pharmacology*,,
559 ISBN: 978-953-51-0222-9
560 Fasinu, P., Viness Pillay, V., Ndesendo, V.M.K., Du Toit, L.C., and Choonara Y.E. (2011). Diverse
561 approaches for the enhancement of oral drug bioavailability. *Biopharmaceutics and drug*
562 *disposition*, 32, 185-209
563 Fen-Lin, W., Razzaghi A., and Souney, P.F. (1993). Seizure after lidocaine for bronchoscopy: case
564 report and review of the use of lidocaine in airway anesthesia. *Pharmacotherapy,* 13, 72-78

565 Ferrari, M., Desai, T., and Bhatia, S. (2007). BioMEMS and Biomedical Nanotechnology. Vol. 3.
566 New York: Springer.
567 Gill, H.S., and Prausnitz, M.R. (2007). Coated microneedles for transdermal delivery. *Journal of*
568 *Controlled Release*, 117, 227-237.
569 Giudice E.L., and Campbell, J.D. (2006). Needle-free vaccine delivery. *Advanced Drug Delivery*
570 *Reviews*, 58, 68-89.
571 Ghosh, P., Brogden, N.K., and Stinchcomb, A.L. (2013a). Effect of formulation pH on transport of
572 naltrexone species and pore closure in microneedle-enhanced transdermal drug delivery.
573 *Molecular Pharmaceutics*, 10, 2331-2339.
574 Ghosh, P., Pinninti, R.R., Hammell, D.C., Paudel, K.S., and Stinchcomb, A.L. (2013b). Development
575 of a codrug approach for sustained drug delivery across microneedle-treated skin. *Journal of*
576 *Pharmaceutical Sciences*, 102, 1458-1467.
577 González-Rodríguez, M.L., Barros, L.B., Palma, J., González-Rodríguez, P.L., and Rabasco A.M.
578 (2007). Application of statistical experimental design to study the formulation variables
579 influencing the coating process of lidocaine liposomes. *International Journal of Pharmaceutics,*
580 337, 336-345.
581 Grossman J.I., Cooper J.A., Frieden J. (1969) Cardiovascular effects of infusion of lidocaine on
582 patients with heart disease. The American Journal of Cardiology, 24, 191-197.
583 Guo, L., Qiu, Y., Chen. J., Zhang. S., Xu, B., and Gao, Y. (2013). Effective transcutaneous
584 immunization against hepatitis B virus by a combined approach of hydrogel patch formulation
585 and microneedle arrays. *Biomedical Microdevices*. DOI 10.1007/s10544-013-9799-z.
586 Gupta, K.C., and Ravi Kumar, M.N.V. (2000). Semi-interpenetrating polymer network beads of
587 crosslinked chitosan–glycine for controlled release of chlorphenramine maleate**.** *Journal of*
588 *Applied Polymer Science,* 76, 672–683.
589 Han, T., and Das, D.B. (2013). Permeability enhancement for transdermal delivery of large molecule
590 using low frequency sonophoresis combined with microneedles, *Journal of Pharmaceutical*
591 *Sciences*, 102 (10), 3614-3622
592 Hedge, N.R., Kaveri, S.V., and Bayry, J. (2011). Recent advances in the administration of vaccines
593 for infectious diseases: microneedles as painless delivery devices for mass vaccination. *Drug*
594 *discovery today*, 16, 1061-1068.
595 Herwadkar, A., Sachdeva, V., Taylor, L.F., Silver, H., and Banga, A.K. (2012). Low frequency
596 sonophoresis mediated transdermal and intradermal delivery of ketoprofen. *International*
597 *Journal of Pharmaceutics,* 423, 289-296.
598 Huet, P.M., and Lelorier, J. (1980). Effects of smoking and chronic hepatitis B on lidocaine and
599 indocyanine green kinetics. *Clinical pharmacology and therapeutics,* 28, 208-215.
600 Hynynen, K. (2010). MRI-guided focused ultrasound treatments, *Ultrasonics*, 50, 221–229
601 Igaki, M., Higashi, T., Hamamoto, S., Kodama, S., Naito, S., and Tokukara. S. (2013). A study of the
602 behavior and mechanism of thermal conduction in the skin under moist and dry heat
603 conditions. *Skin Research and Technology*, 0, 1-7.

Ito, Y., Ohta, J., Imada, K., Akamatsu, S., Tsuchida, N., Inoue, G., Inoue, N., Takada, K. Dissolving microneedles to obtain rapid local anesthetic effect of lidocaine at skin tissue (2013) *Journal of Drug Targeting*, 21, 770-775.

Kalluri. H, and Banga, A. (2011). Transdermal delivery of proteins. *AAPS PharmSciTech*, 12, 431-441.

Kim, Y., Park, J., and Prausnitz, M.R. (2012). Microneedles for drug and vaccine delivery. *Advanced Drug Delivery Reviews*, 64, 1547-1568.

Kochhar, J.S., Lim, W.X.S., Zou, S., Foo, W.Y., Pan, J., Kang, L. Microneedle integrated transdermal patch for fast onset and sustained delivery of lidocaine (2013) *Molecular Pharmaceutics*, 10, 4272-4280.

Kwon, S.Y. (2004). In vitro evaluation of transdermal drug delivery by a micro-needle patch. *Controlled Release Society 31st Annual Meeting Transactions*. *TheraJect Inc*. no. 115.

Lastumäki, T.M., Lassila, L.V.J., and Vallittu, P.K. (2003). The semi-interpenetrating polymer network matrix of fibre-reinforced composite and its effect on the surface adhesive properties. *Journal of Materials Science-Materials in Medicine*, 14, 803-809.

Li, X., Zhao, R., Qin, Z., Zhang, J., Zhai, S., Qiu, Y., Gao, Y., Xu, B., and Thomas, S,H. (2010). Microneedle pretreatment improves efficacy of cutaneous topical anesthesia. *American Journal of Emergency Medicine,* 28, 130-134.

Li, X.-G., Zhao, R.-S., Qin, Z.-L., Gao, Y.-H., Zhang, J., Zhai, S.-D., Xu, B. Painless microneedle transdermal patch enhances permeability of topically applied lidocaine (2008) *Chinese Journal of New Drugs*, 17 (7), pp. 597-601. Merino, G., Kalia, Y.N., Delgado-Charro, M.B., Potts, R.O., and Guy, R.H. (2003). Frequency and thermal effects on the enhancement of transdermal transport by sonophoresis. *Journal of Controlled Release*, 88, 85-94.

Milewski, M., and Stinchcomb, A. (2011). Vehicle composition influence on the microneedle-enhanced transdermal flux of naltrexone hydrochloride. *Pharmaceutical Research,* 28, 124–134.

Mitragotri, S. (2013). Devices for overcoming biological barriers: The use of physical forces to disrupt the barriers. *Advanced Drug Delivery Reviews*, 65, 100-103.

Mitragotri, S., and Kost, J. (2004). Low-frequency sonophoresis: A review. *Advanced Drug Delivery Reviews*, 56, 589-601.

Naik. A., Kalia, Y.N., and Guy, R.H. (2000). Transdermal drug delivery: overcoming the skin's barrier function. *Pharmaceutical Science and Technology Today*, 3, 318-326.

Nayak, A., Das, D.B., and Vladisavljević, G.T. (2013). Microneedle assisted permeation of lidocaine carboxymethylcellulose with gelatine co-polymer hydrogel. *Pharmaceutical Research*. DOI: 10.1007/s11095-013-1240-z (in press)

Nayak, A., and Das D. (2013). Potential of biodegradable microneedles as a transdermal delivery vehicle for lidocaine. *Biotechnolology Letters*, 35, 1351–1363

642 Olatunji, O, Das, DB, Nassehi, V (2012) Modelling transdermal drug delivery using microneedles:
643 Effect of geometry on drug transport behaviour, *Journal of Pharmaceutical Sciences*, 101(1),
644 pp.164-175, ISSN: 0022-3549. DOI: 10.1002/jps.22736.
645 Olatunji, O., Das, D.B., Garland, M.J., Belaid, L., and Donnelly, R.F. (2013). Influence of array
646 interspacing on the force required for successful microneedle skin penetration: theoretical and
647 practical approaches. *Journal of Pharmaceutical Sciences***,** 102, 1209-1221.
648 Olatunji, O, Igwe, CC, Ahmed, AS, Alhassan, OA, Asieba, GO, **Das, DB** (2014) Microneedles from
649 fish scale biopolymer, *Journal of Applied Polymer Science*, DOI: 10.1002/app.40377 (in
650 press).
651 Park, N., Kwon, B., Kim, I.S., and Cho, J. (2005). Biofouling potential of various NF membranes with
652 respect to bacteria and their soluble microbial products (SMP): Characterizations, flux decline,
653 and transport parameters. *Journal of Membrane Science*, 258, 43-54.
654 Polat, B., Hart, D., Langer, R., and Blankschtein, D. (2011). Ultrasound-mediated transdermal drug
655 delivery: mechanisms, scope, and emerging trends. *Journal of Controlled Release*, 152, 330-
656 348.
657 Richards, N., and McMahon, S.B. (2013). Targeting novel peripheral mediators for the treatment of
658 chronic pain. *British Journal of Anaesthesia,* 111 (1), 46-51.
659 Roxhed, N., Gasser T.C., Griss, P. (2007) Penetration-enhanced ultrasharp microneedles and
660 prediction on skin intereation for efficient transdermal drug delivery. Journal of
661 microelectromechanical systems, 16, 1429-1440.
662 Rudin, N.J. (2013). Topical analgesics for chronic pain. *Current Physical Medicine and*
663 *Rehabilitation Reports*. DOI 10.1007/s40141-013-0028-8.
664 Scarfone, R.J., Jasani, M., and Gracely, E.J. (1998). Pain of Local Anesthetics: Rate of
665 Administration and Buffering. *Annals of Emergency Medicine*, 31 (1), 36-40
666 Schulz, M., Iwersen-Bergmann, S., Andresen, H., and Schmoldt, A. (2012). Therapeutic and toxic
667 blood concentrations of nearly 1,000 drugs and other xenobiotics. Critical Care, 16, R136
668 Sekkat, N., Kalia, Y.N., Guy, R.H. (2004). Porcine ear skin as a model for the assessment of
669 transdermal drug delivery to premature neonates. *Pharmaceutical Research*, 21, 1390-1397.
670 Shah, U.U., Roberts. M., Orlu Gul, M., Tuleu, C., and Beresford, M.W. (2011). Needle-free and
671 microneedle drug delivery in children: A case for disease-modifying antirheumatic drugs
672 (DMARDs). *International Journal of Pharmaceutics*, 416,1-11.
673 Shipton, E.A. (2012). Advances in delivery systems and routes for local anaesthetics. *Trends in*
674 *Anaesthesia and Critical Care*, 2, 228-233.
675 Sze, A., Erickson, D., Ren, L., Li, D. (2003). Zeta-potential measurement using the Smoluchowski
676 equation and the slope of the current-time relationship in electroosmotic flow. *Journal of*
677 *Colloid and Interface Science*, 261, 402-410.
678 Wilson, J.R., Kehl, L.J., Beiraghi, S.
679 (2008). Enhanced topical anesthesia of 4% lidocaine with microneedle pretreatment and
680 iontophoresis. *Northwest dentistry*, 87, 40-41.

681 Wolloch L, Kost J (2010) The importance of microjet vs shock wave formation in sonophoresis.
682 Journal of Controlled Release, 148, 204-211.
683 Xu, R., Wu, C., and Xu, H. (2007). Particle size and zeta potential of carbon black in liquid media.
684 *Carbon*. 45 :2806–2809
685 Zhang, Y., Brown, K., Siebenaler, K., Determan, A., Dohmeier, D., and Hansen, K. (2012).
686 Development of lidocaine-coated microneedle product for rapid, safe, and prolonged local
687 analgesic action. *Pharmaceutical Research*, 29, 170-177.
688 Zhang, Y., Siebenaler, K., Brown, K., Dohmeier, D., and Hansen, K. (2012). Adjuvants to prolong
689 the local anesthetic effects of coated microneedle products. *International Journal of*
690 *Pharmaceutics*, 439, 187-192.
691 Zhang, D, Das, DB, Rielly, CD (2014) Potential of microneedle-assisted micro-particle delivery by
692 gene guns: a review, *Drug Delivery*, DOI: 10.3109/10717544.2013.864345.
693 Zhao, Y., Kang, J., and Tan, T. (2006). Salt-, pH- and temperature-responsive semi-interpenetrating
694 polymer network hydrogel based on poly(aspartic acid) and poly(acrylic acid). *Polymer*, 47,
695 7702-7710.

Table 1

Lidocaine NaCMC/gel hydrogel mass ratio with particle size values

Sample ID	NaCMC (% w/v)	Gelatine (c % w/w)	Lidocaine (% w/w)	NaCMC:Gelatine ratio	Drier Type	Mean Particle Diameter ± S.D. (μm)	Particle Diameter range (μm)
F1	1.2	2.0	2.4	1:1.6	Vacuum	5.89 ± 0.0026	1 - 13
F2	1.2	2.4	2.4	1:2.00	Vacuum	6.04 ± 0.0027	1 - 14
F3	1.2	2.8	2.4	1:2.33	Vacuum	6.81 ± 0.0029	2 - 17
F4	1.2	3.2	2.4	1:2.67	Vacuum	7.42 ± 0.0029	3 - 17
F5	1.2	3.2	2.4	1:2.67	Rotary	14.60 ± 0.0067	4 - 31

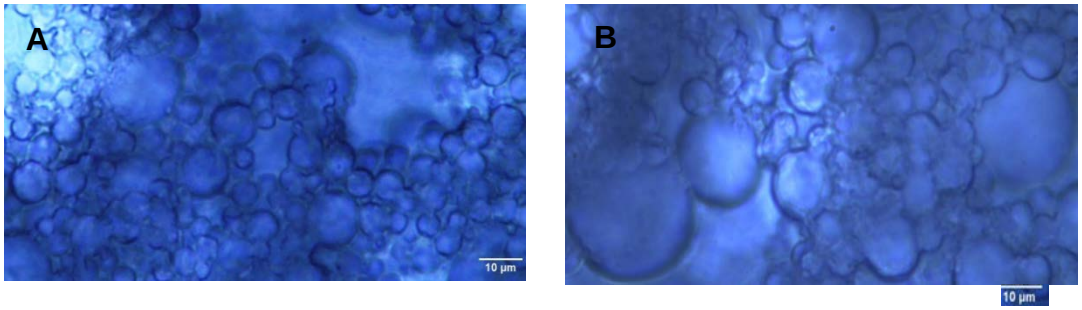

Fig. 1. Micrograph of **a.** lidocaine NaCMC;gel 1:2.33 hydrogel showing distinctly formed microparticles. **b.** lidocaine NaCMC:gel 1:2.66 hydrogel showing larger and slightly more agglomerated microparticles.

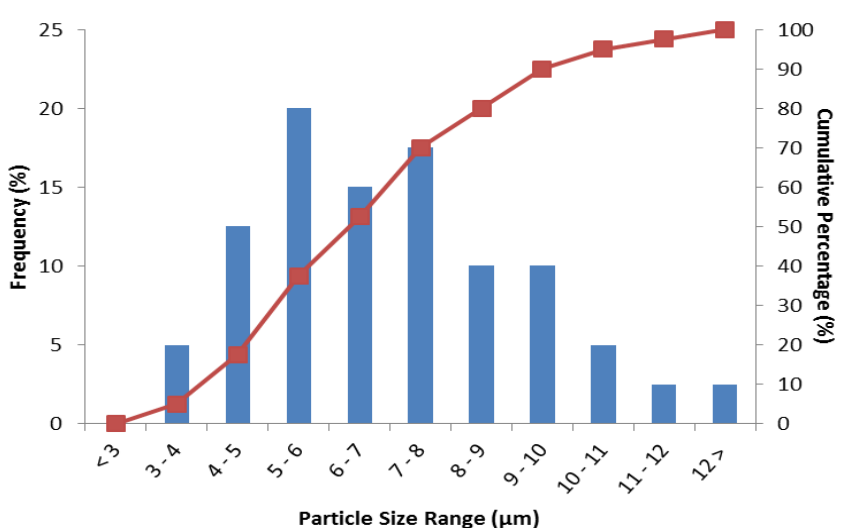

Fig. 2. Particle size distribution of Lidocaine NaCMC/gel hydrogels

702

703

704

705

706

707

708

709

710

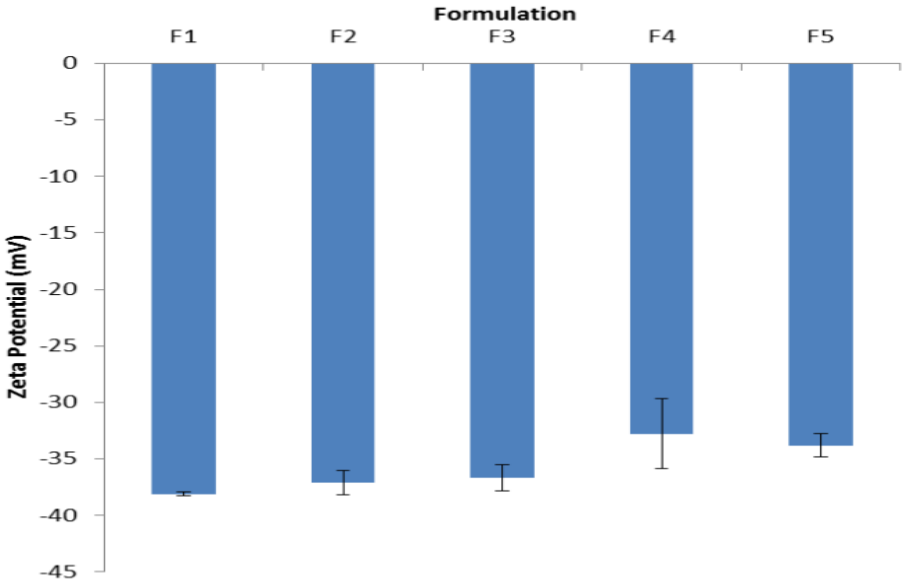

Fig. 3. Lidocaine NaCMC/GEL 1:1.6 to 1:2.66 (F1 to F4) and lidocaine NaCMC/GEL1:2.66 by rotary evap prep. (F5) for zeta potential

711

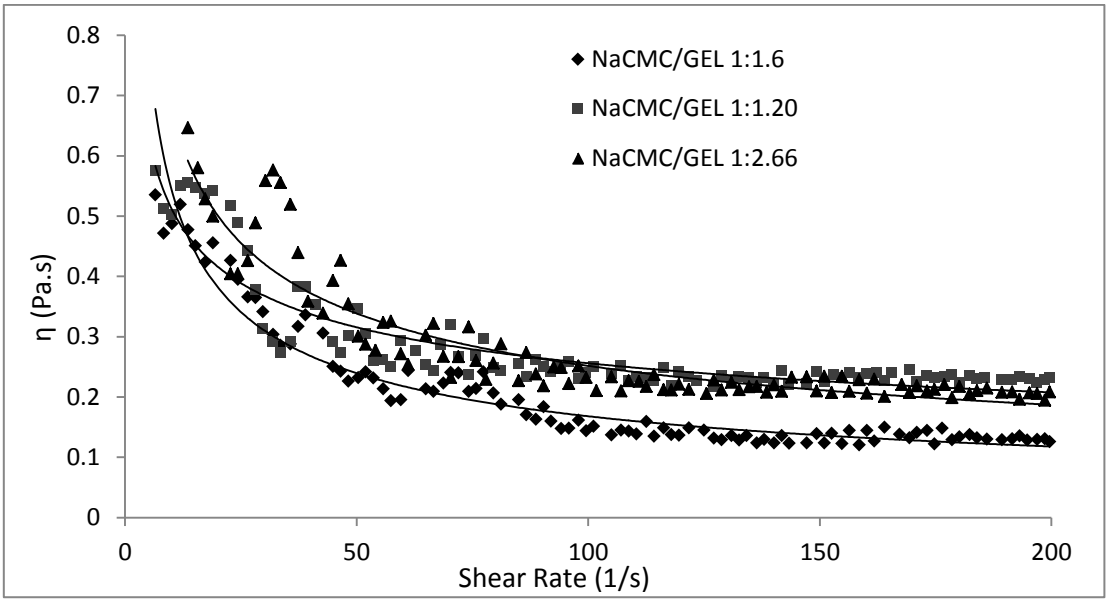

Fig. 4. Lidocaine 2.44 % w/w NaCMC/GEL ratio pseudoplasticity

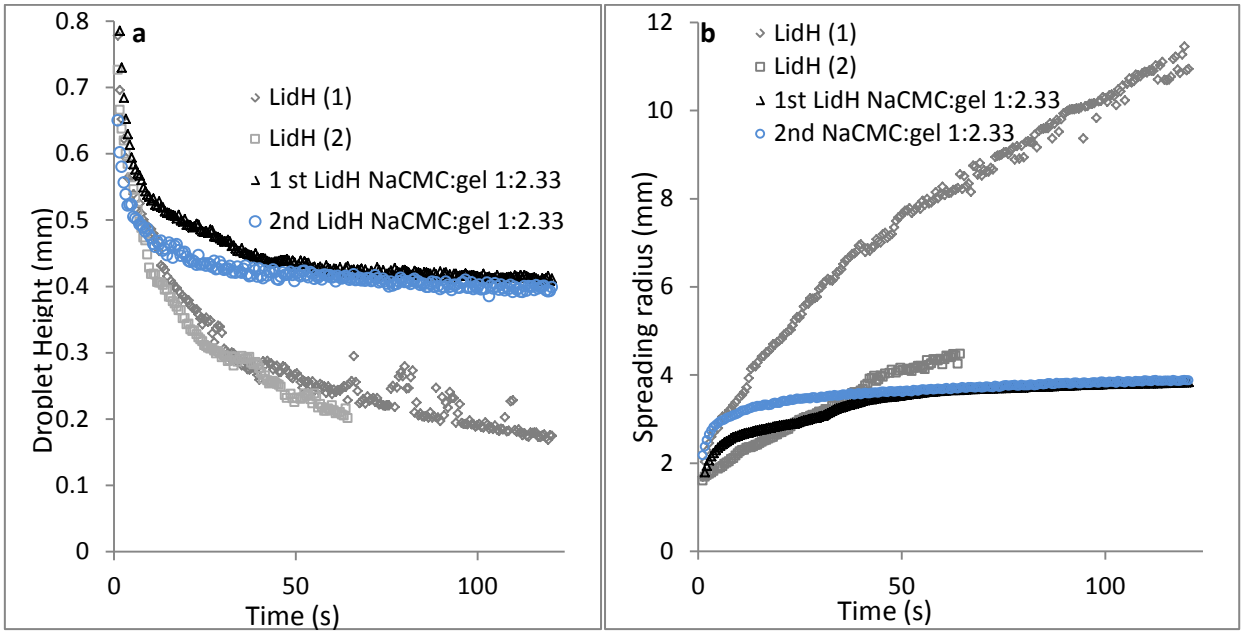

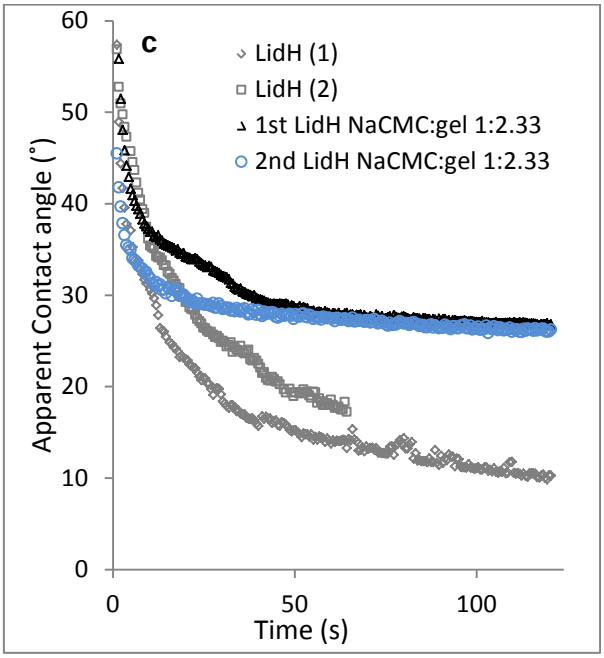

Fig. 5 Lidocaine NaCMC/gel 1:2.33 comparison with Newtonian lidocaine solution according to **a.** droplet heights **b.** spreading radii **c.** apparent contact angles. The results suggest that the spreading of lidocaine NaCMC/gel 1:2.33 on the skin surface is much more predictable/controllable as compared to lidocaine solution.

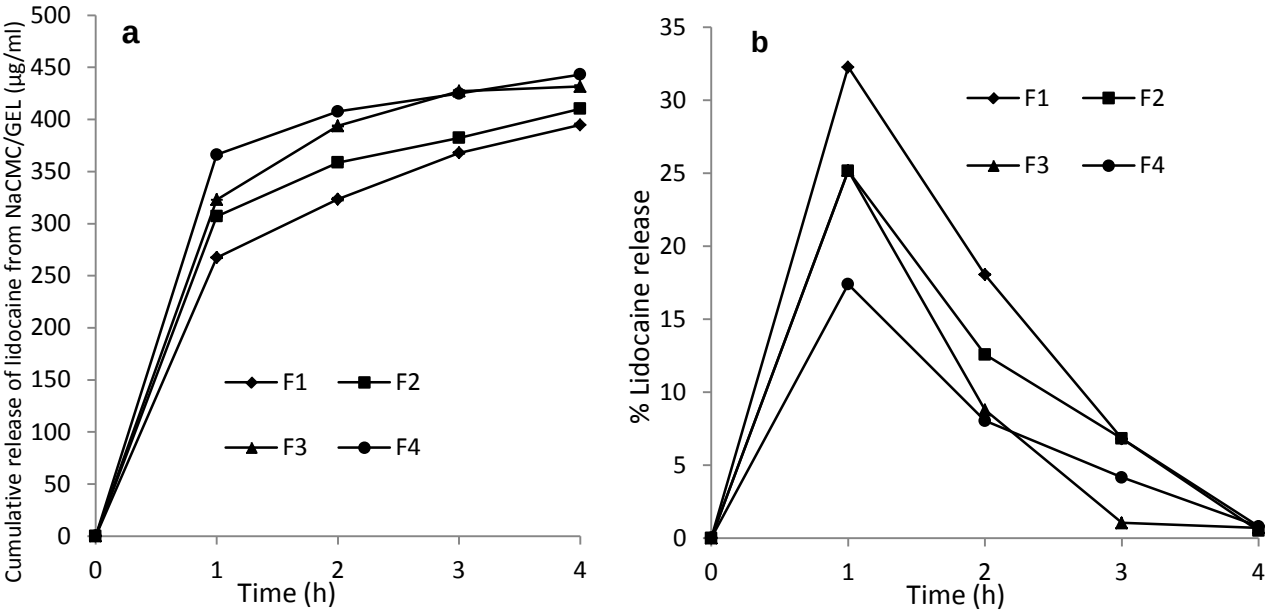

737

738 **Fig. 6.** The controlled release of Lidocaine 2.44% w/w encapsulated **a.** NaCMC/GEL 1:1.6 (F1), NaCMC/GEL 1:2.0 (F2), NaCMC/GEL 1:2.33 (F3) and NaCMC/GEL 1:2.66 (F4) **b.** as a percentage into DI water medium from NaCMC/GEL 1:1.6 (F1), NaCMC/GEL 1:2.0 (F2), NaCMC/GEL 1:2.33 (F3) and NaCMC/GEL 1:2.66 (F4). The error

739 bars in a) the standard deviation of mean represents the error. b) No error bars indicated

740

741

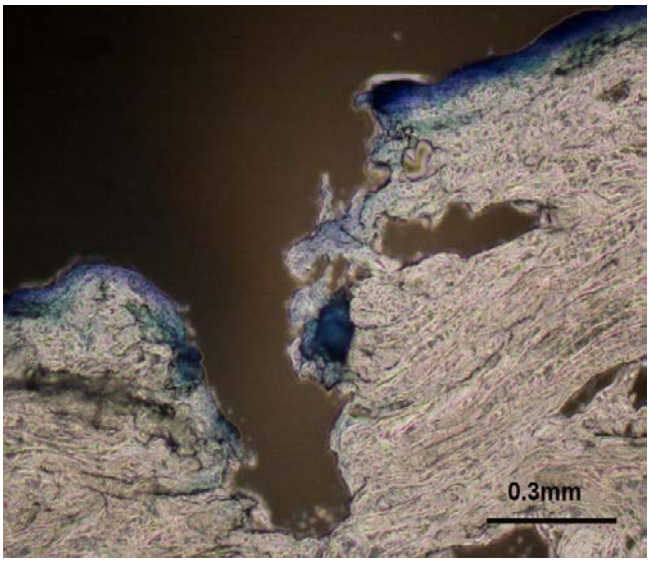

742

743 **Fig. 7** The microneedle insertion depth of skin sample using 1100 µm microneedles under thumb
744 pressure. The histological studies shows that although the microneedles are 1100 µm, for the
745 microneedle density in the array and force applied, they creates holes of approximately 400 µm.

746

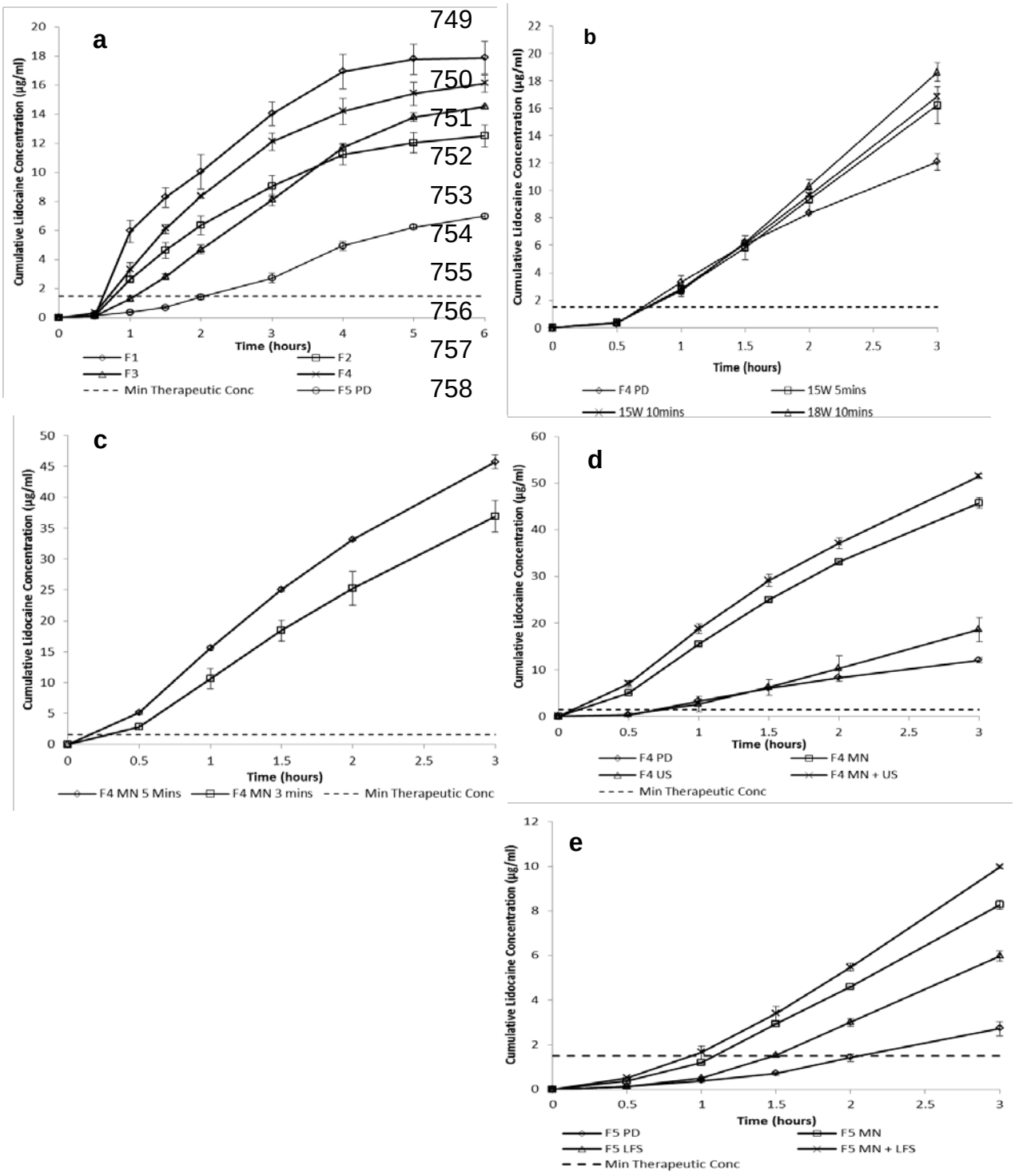

Fig. 8. Cumulative lidocaine permeation from Lidocaine. **a** NaCMC/GEL 1:1.6 (F1), NaCMC/GEL 1:2.0 (F2), NaCMC/GEL 1:2.33 (F3), NaCMC/GEL 1:2.66 (F4) and passive diffusion (PD) NaCMC/GEL 1:2.66 by rotor evaporation prep stage (F5). **b** F4 PD and comparative pre-treatment with ultrasound at 15W and 18W for 5 and 10 minutes respectively. **c** F4 adapting a microneedle (MN) patch for a 3 minute and 5 minute pre-treatment duration for Lidocaine NaCMC/GEL 1:2.66. **d** F4 adapting NaCMC/GEL 1:2.66 (F4 PD), NaCMC/GEL 1:2.66 (F4 US, 18W 10min.), NaCMC/GEL 1:2.66 (F4 MN, 5 min.) and NaCMC/GEL 1:2.66 (F4 MN 5 min and US 18W 10min). **e** NaCMC/GEL 1:2.66 (F5 PD), NaCMC/GEL 1:2.66 (F5 LFS, 18W 10min.), NaCMC/GEL 1:2.66 (F5 MN, 5 min.) and NaCMC/GEL 1:2.66 (F5 MN 5 min, LFS, 18W 10min).

776

777

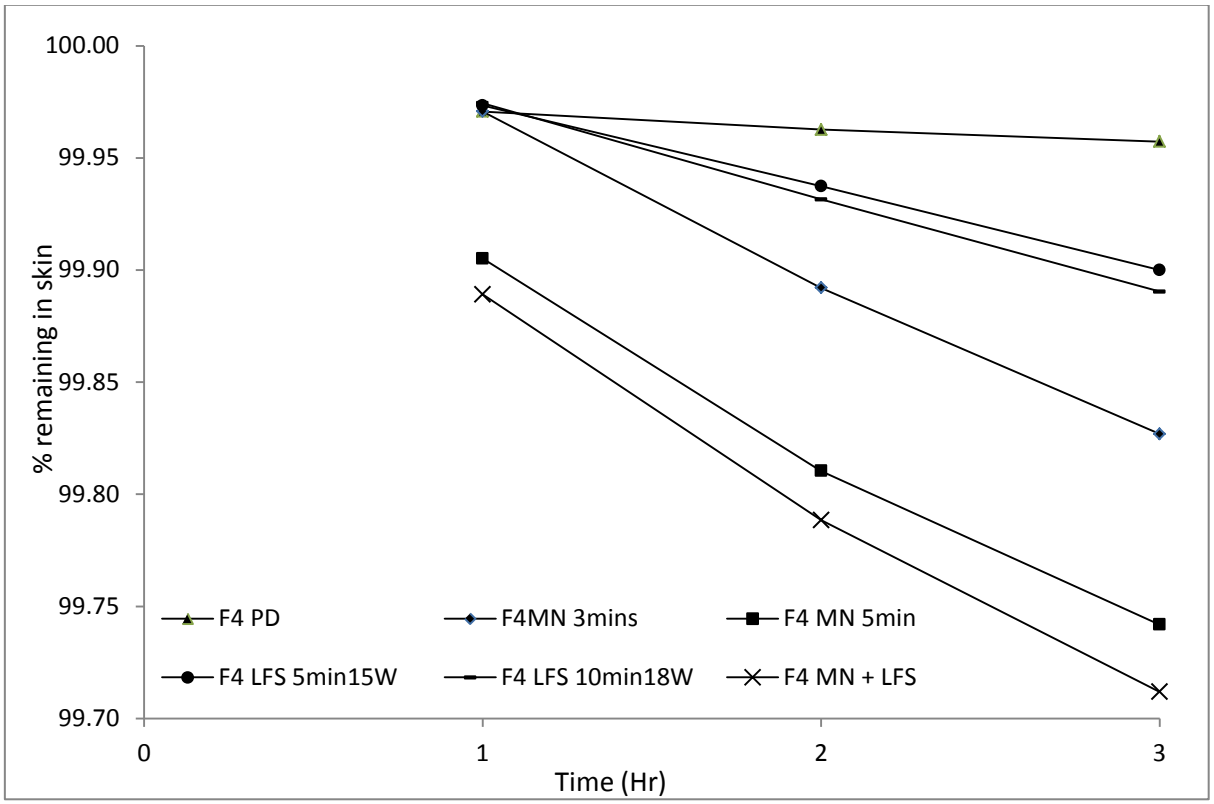

778

779 **Fig. 9.** Percentage of lidocaine contained in (F4) NaCMC/GEL 1:2.66 (▲Passive Diffusion), (◆ microneedles, 3 min),
780 (■ microneedles, 5 min.), (● LFS 5 min 15W), (▬ LFS 10 min 18W), (✖ MN + LFS). (Error bars outline a
781 random error range of 0.005 %)